ARI The Bulletin of the Istanbul Technical University VOLUME 54, NUMBER 1
Communicated by Derin Orhon

The New Generation Transition Curves

Ergin Tarı
Department of Geodesy and Photogrammetry Engineering, Surveying Techniques Division, Civil Engineering Faculty, Istanbul Technical University, 34469 Maslak, Istanbul, Turkey
(Received 13 April 2003)

The necessity for the curves, which have much better vehicle-road dynamical properties, has arisen since the last quarter of the 20^{th} century, because the speed used especially on the railways was increased. Although the dominance of the spiral curve as a transition curve has been still in progress by means of the common and wide knowledge base and infrastructure such as lots of ready to use software and the traditional rules of the responsible facilities, many investigations have been carried out on developing new curves, which can be used for the design of horizontal geometry and have many advantages with respect to road dynamics, because the spiral curve has been realized that it is not adequate for the road dynamics. So the transition curves superior for road dynamics have been invented by using the properties of vehicle-road dynamics, represented by the function of lateral change of acceleration that is the most important criteria to evaluate the curves in this manner. The recently invented superior curves can be considered as Sinusoidal curve, Baykal curve, Tarı-1 curve, and Tarı-2 curve. Sinusoidal curve is a known and applied curve joining a straight line with a circular arc by providing the condition of second-degree contact related with properties of vehicle-road dynamics. Baykal curve is a fundamental curve joining two straight lines without the necessity of a circular arc and it is the first realization of the new generation curves mentioned in the paper. Tarı-1 curve is a new curve joining a straight line with a circular arc by providing the condition of second-degree contact. Tarı-2 curve is a superior implementation of Baykal curve by providing the condition of second-degree contact. In this paper, each of these curves has been examined by using the function of lateral change of acceleration in motion model with constant velocity.

Keywords: Transition curve, lateral change of acceleration, vehicle road dynamics, railway curve, highway curve motion model

1. Introduction

In the past, using a circular curve simply solved the problem of joining two straight lines on railway or highway alignments. This simplicity had been widely used before high speeds became necessary. However, with increased speed requirements especially on the railways, the implementations of the circular curve were examined [1-3]. These examinations resulted in the use of the transition curves between straight lines and a circular arc including circles with a 2R radius and cubic parabola [4]. Computationally more complicated curves (e.g. spiral curve) have been used as a result of developments in calculation techniques [5]. The spiral curve as a transition curve is still the most widely used, because of wide knowledge base, infrastructure, the existence of ready to use software, and the traditional rules of the responsible agencies.

The necessity for the curves, which have much better vehicle-road dynamical properties, has arisen since the last quarter of the 20^{th} century. Curves such as the ones in [6-10], were discovered, although some of them based their curves on the incorrect comparison criteria as shown in detail by Baykal [11]. The first realistic curve in the application of the transition curves with base of traditional lateral change of acceleration function is the sinusoidal curve [12]. The new lateral change of acceleration function derived in [11] has suggested changing the design criterion and depending on these suggestions new transition curves have proposed. The new generation transition curves began with [13] and continued with [14-16] and [17]. These curves are generally based on the basics of the function of the lateral change of acceleration presented in [11]. The Baykal curve given in [18] was a radical new transition curve in the transition curve manner. The Tarı-1 curve presented in [17] is another radical example of the new transition curve family, especially by the reason of combining road elements with the second-degree contact. The Tarı-1 curve is a transition curve joining a straight line with a circular arc. It was proved to be a superior alternative to curves such as Spiral, Bloss and

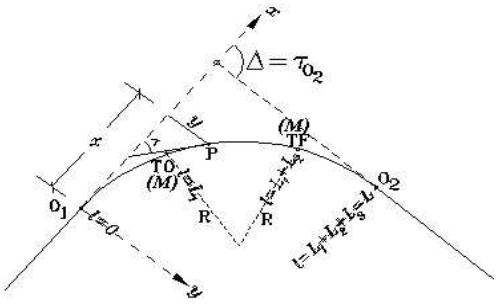

Figure 1. Horizontal geometry of curves with setting out elements.

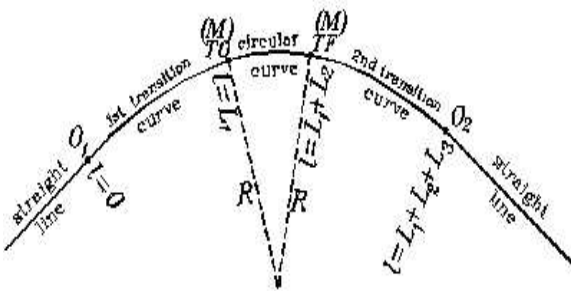

Figure 2. Horizontal geometry of the compound curves.

Sinuzoidal curves [15, 17].

In this study, 4 new generation transition curves with lateral change of acceleration functions are given briefly. The sinusoidal curve, the Baykal curve, the Tarı-1 curve, and the Tarı-2 curve is then examined by means of lateral change of acceleration function in motion model with constant velocity. Each curve is explained with a few words and basic equations.

2. Lateral Change of Acceleration (LCA)

The LCA is the most important criterion determining the conformity of horizontal geometry of route related to the vehicle-road dynamics [6, 11, 12, 15, 17, 18, 19]. Older derivations of LCA functions [20-23] differ and are even incorrect in some cases [7, 9, 24, 25] as explained in [11].

The LCA is the change of the resultant acceleration occurring along the curve normal with respect to time. The resultant acceleration is formed by the free forces acting on a vehicle with a mass (m) and an instantaneous velocity (v), moving on a curve orbit. The equation of LCA is given as [11]

$$z = \frac{da}{dT}\hat{n} = \frac{pv}{\sqrt{u^2+p^2}} \times \left\{ 3ka_t + v^2\frac{dk}{dl} - \frac{kv^2u+gp}{u^2+p^2}\frac{du}{dl} \right\} \quad (1)$$

where z is the lateral change of acceleration (LCA) [m/sec^3], a is the resultant acceleration formed by free forces [m/sec^2], T is time [sec], ν is vehicle speed [m/sec], a_t is tangential acceleration produced by motor force [m/sec^2], p is the horizontal width of the road platform [m], u is the superelevation which is the amount of elevation of the outer side according to inner side[m], k is curvature of orbiting curve path defined on horizontal plane [1/m], g is gravity constant [9.81 m/sec^2], l is arc length measured from a chosen point on the route (natural parameter)[m], n is unit vector along the curve normal.

If three functions, $v = v(l)$ = function of velocity related to the road, $k = k(l)$ = function of curvature related to the road, $u = u(l)$ = function of superelevation related to the road, are known, the function of LCA given by (1) can be derived for any curve.

3. The New Generation Transition Curves

In order to calculate setting out elements of curves mentioned in this paper, the relationship between the local cartesian coordinates of any point, x and y, and the angles, τ and Δ (Fig. 1) is required. The origin of local system is at O_1 in Fig. 1 and axes are in the direction of x and y as indicated in the figure. Details of these calculations are given in [15] and overall equations for the calculations can be found in [8, 26, 27]. The suggestion for the solution method is to use a numerical integration technique and the technique is suggested as Romberg Integration Method [8, 14, 28, 29, 30].

The new generation transition curves can be divided in two groups. The first group contains compound curves which are formed by straight line - 1^{st} transition curve - circular arc - 2^{nd} transition curve - straight line given in Fig. 2. The characteristic points in the form of compound curves are O_1, TO, TF, and O_2. The radius of the

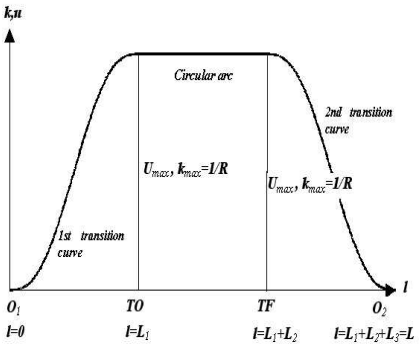

Figure 3. The curvature and superelevation diagrams of the compound curves.

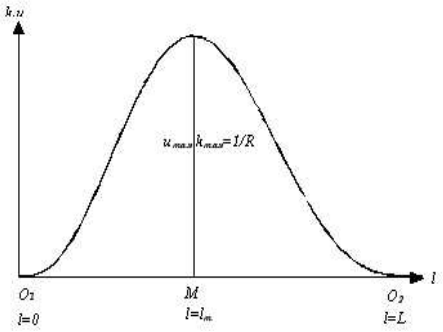

Figure 4. The curvature and superelevation diagrams of the continuous curves.

circular curve is R at the points of TO and TF which are the points two elements join together. These joining points as well as O1 and O2 are essential points in the examination of LCA diagrams. The model diagrams of curvature and superelevation functions of compound curves are given in Fig. 3 where u_{max} is the maximum value of the superelevation and k_{max} is the maximum value of the curvature. The sinusoidal curve and the Tarı-1 curve reside in the first group.

The second group contains the curves join two straight lines without a circular arc. Transition curves joining two straight lines without a circular arc are proposed by means of better properties related to road-vehicle dynamics, starting with [13]. These transition curves have a total length of L and have a specific point M at which the radius of curvature is R and the arc length of the point M from the beginning of the curve is l_M (Fig. 1 and Fig. 4). The characteristic points in these types of curves are O_1, M, and O_2. The model diagrams of curvature and superelevation functions of this second group of curves are given in Fig. 4. The Baykal curve and the Tarı-2 curve belong to this second group.

3.1. Sinusoidal Curve

Sinusoidal curve joins a straight line with a circular arc by providing the second degree contact [12]. The curvature function of the sinusoidal curve is derived from sinus function as

$$k_s(l) = \frac{1}{R}\left(\frac{l}{L} - \frac{1}{2\pi}\sin(2\pi\frac{l}{L})\right) \tag{2}$$

By applying the boundary conditions

$$l = 0 \Rightarrow k = 0 \ and \ k' = 0 \tag{3}$$

$$l = L_1 \Rightarrow k = 1/R \ and \ k' = 0 \tag{4}$$

The curvature function of the first sinusoidal curve in the form of compound curve is obtained as

$$k_{s,1}(l) = \frac{1}{R}\left(\frac{l}{L_1} - \frac{1}{2\pi}\sin(\frac{l}{L_1}2\pi)\right), \quad 0 \le l \le L_1 \tag{5}$$

The curvature function of the circular arc is

$$k_{s,2}(l) = \frac{1}{R} = constant, \quad L_1 \le l \le L_1 + L_2 \tag{6}$$

With the boundary conditions as

$$l = L_1 + L_2 \Rightarrow k = 1/R \ and \ k' = 0 \tag{7}$$

$$l = L_1 + L_2 + L_3 \Rightarrow k = 0 \ and \ k' = 0 \tag{8}$$

The curvature function of the second sinusoidal curve is

$$k_{s,3}(l) = \frac{1}{R}\left(\frac{(L-l)}{L_3} - \frac{1}{2\pi}\sin(\frac{(L-l)}{L_3}2\pi)\right), \quad L_1 + L_2 \le l \le L \tag{9}$$

The superelevation functions can be obtained by taking into account of similar boundary conditions for curvature functions

$$u_{s,1}(l) = u_{max}\left(\frac{l}{L_1} - \frac{1}{2\pi}\sin(\frac{l}{L_1}2\pi)\right), \quad 0 \le l \le L_1 \tag{10}$$

$$u_{s,2}(l) = u_{max} = constant,\ L_1 \le l \le L_1+L_2 \quad (11)$$

$$u_{s,3}(l) = u_{max}\left(\frac{(L-l)}{L_3} - \frac{1}{2\pi}\sin(\frac{(L-l)}{L_3}2\pi)\right),$$
$$L_1 + L_2 \le l \le L \quad (12)$$

3.1.1. LCA Function of Sinusoidal Curve in Motion Model with Constant Velocity

In the motion model with constant velocity, velocity (ν) is assumed to be constant ($a_t = 0$) along the transition curve in Eq. 1. The LCA function of the first sinusoidal curve part in the compound curve can be obtained by using Eq. 5, Eq. 10 and their derivatives with respect to l in Eq. 1.

$$z_{s,1}(t) = \frac{N_{s,1}\nu(\nu^2 - gR\tan\alpha_m)}{R(1+Q_{s,1}^2\tan^2\alpha_m)^{3/2}},$$
$$0 \le t \le \frac{L_1}{L} \quad (13)$$

where

$$t = l/L \quad (14)$$

$$Q_{s,1} = \frac{Lt}{L_1} - \frac{1}{2\pi}\sin(\frac{Lt}{L_1}2\pi),$$
$$N_{s,1} = \frac{1}{L_1} - \frac{1}{L_1}\cos(\frac{Lt}{L_1}2\pi) \quad (15)$$

The LCA function of the circular arc is obtained by using Eq. 14, Eq. 6, and Eq. 11 in Eq. 1

$$z_{s,2}(t) = 0,\ \frac{L_1}{L} \le t \le \frac{L_1+L_2}{L} \quad (16)$$

The LCA function of the second sinusoidal part is derived by using Eq. 14, Eq. 9, and Eq. 12 with derivatives with respect to l in Eq. 1 as

$$z_{s,3}(t) = \frac{N_{s,2}\nu(\nu^2 - gR\tan\alpha_m)}{R(1+Q_{s,2}^2\tan^2\alpha_m)^{3/2}},$$
$$\frac{L_1+L_2}{L} \le t \le 1 \quad (17)$$

where

$$Q_{s,2} = \frac{L-Lt}{L_3} - \frac{1}{2\pi}\sin\left(\frac{L-Lt}{L_3}2\pi\right),$$
$$N_{s,2} = -\frac{1}{L_3} + \frac{1}{L_3}\cos\left(\frac{L-Lt}{L_3}2\pi\right) \quad (18)$$

The extensive derivations of the equations about the sinusoidal curve and LCA functions of the sinusoidal curve can be found in [15].

3.2. Baykal Curve

The Baykal curve joins the two straight lines with a single curve. The arc length of the point M from the beginning of the curve is $l_m \cong 0.558$L (Fig. 1 and Fig. 4). The curvature and superelevation functions of the Baykal curve are

$$k_B(t) = \frac{1}{R}(A_B t^5 + B_B t^4 + D_B t^2)$$
$$u_B(t) = u_{max}(A_B t^5 + B_B t^4 + D_B t^2) \quad (19)$$

where t=l/L, A_B ≅15.538, B_B ≅23.307 and D_B ≅7.769 [18].

3.2.1. LCA Function of Baykal Curve in Motion Model with Constant Velocity

The LCA function of the Baykal curve in motion model with constant velocity is derived from Eq. 1 by taking into consideration Eq. 19 as follows:

$$z_B(t) = \frac{\nu N(\nu^2 - gR\tan\alpha_m)}{LR(Q^2\tan^2\alpha_m + 1)^{3/2}},\quad 0 \le t \le 1 \quad (20)$$

where

$$\tan\alpha_m = \frac{u_{max}}{b},$$
$$Q = At^5 + Bt^4 + Dt^2,$$
$$N = 5At^4 + 4Bt^3 + 2Dt \quad (21)$$

The extensive derivations of the equations about the Baykal curve and LCA functions of the Baykal curve can be found in [18].

3.3. Tarı-1 Curve

Tarı-1 curve joins a straight line with a circular arc. The curve provides condition of second degree contact to joining elements, related to the properties of road dynamics [12, 15]. The curvature function of the Tarı-1 curve is suggested to be a function of fifth degree parabola.

$$k(l) = al^5 + bl^4 + cl^3 + dl^2 + el + f \quad (22)$$

The curvature function of the first Tarı-1 curve is suggested to provide the boundary conditions given below

$$l = 0 \Rightarrow k = 0,\ k' = 0,\ k'' = 0,$$
$$l = L_1 \Rightarrow k = 1/R,\ k' = 0, k'' = 0 \quad (23)$$

With these assumptions, curvature function of first Tarı-1 curve in the form of compund curve is obtained as [15]

$$k_{T1,1}(l) = \frac{l^3}{RL_1^3}\left(\frac{6l^2}{L_1^2} - \frac{15l}{L_1} + 10\right), \quad 0 \le l \le L_1 \tag{24}$$

The curvature function of the circular arc with a radius R is

$$k_{T1,2}(l) = \frac{1}{R} = constant,\ L_1 \le l \le L_1 + L_2 \tag{25}$$

The curvature function of the second Tarı-1 curve in the form of compound curve satisfies the conditions given below,

$$\begin{aligned} l &= L_1 + L_2 \Rightarrow k = 1/R, k' = 0, k'' = 0, \quad (26)\\ l &= L_1 + L_2 + L_3 = L \Rightarrow k = 0, k' = 0, k'' = 0 \end{aligned}$$

and

$$k_{T1,3}(l) = \frac{(L-l)^3}{RL_3^3}\left(\frac{6(L-l)^2}{L_3^2} - \frac{15(L-l)}{L_3} + 10\right), \quad L_1 + L_2 \le l \le L_1 + L_2 + L_3 = L \tag{27}$$

is obtained. Similarly, the superelevation functions of the Tarı-1 compound curve can be obtained as

$$u_{T1,1}(l) = \frac{u_{max} l^3}{L_1^3}\left(\frac{6l^2}{L_1^2} - \frac{15l}{L_1} + 10\right), \quad 0 \le l \le L_1 \tag{28}$$

$$u_{T1,2}(l) = u_{max} = constant, \quad L_1 \le l \le L_1 + L_2 \tag{29}$$

$$u_{T1,3}(l) = \frac{u_{max}(L-l)^3}{L_3^3} \times \left(\frac{6(L-l)^2}{L_3^2} - \frac{15(L-l)}{L_3} + 10\right), \quad L_1 + L_2 \le l \le L_1 + L_2 + L_3 = L \tag{30}$$

3.3.1. LCA Function of Tarı-1 Curve in Motion Model with Constant Velocity

For the first Tarı-1 curve part, introducing Eq. 24, Eq. 28 and derivatives of them into Eq. 1

$$z_{T1,1}(t) = \frac{N_{T1,1}\nu(\nu^2 - gR\tan\alpha_m)}{R(1 + Q_{T1,1}^2\tan^2\alpha_m)^{3/2}}, \quad 0 \le t \le \frac{L_1}{L} \tag{31}$$

where

$$\begin{aligned} Q_{T1,1} &= \frac{6L^5t^5}{L_1^5} - \frac{15L^4t^4}{L_1^4} + \frac{10L^3t^3}{L_1^3},\\ N_{T1,1} &= \frac{30L^4t^4}{L_1^5} - \frac{60L^3t^3}{L_1^4} + \frac{30L^2t^2}{L_1^3} \end{aligned} \tag{32}$$

can be derived.

For the circular arc, introducing Eq. 25, Eq. 29 and derivatives of them into Eq. 1

$$z_{T1,2}(t) = 0, \quad \frac{L_1}{L} \le t \le \frac{L_1 + L_2}{L} \tag{33}$$

can be derived.

For the second Tarı-1 curve introducing Eq. 27, Eq. 30 and derivatives of them into Eq. 1

$$z_{T1,3}(t) = \frac{N_{T1,2}\nu(\nu^2 - gR\tan\alpha_m)}{R(1 + Q_{T1,2}^2\tan^2\alpha_m)^{3/2}}, \quad \frac{L_1 + L_2}{L} \le t \le 1 \tag{34}$$

where

$$\begin{aligned} Q_{T1,2} &= \frac{6(L-Lt)^5}{L_3^5} - \frac{15(L-Lt)^4}{L_3^4} + \frac{10(L-Lt)^3}{L_3^3},\\ N_{T1,2} &= -\frac{30(L-Lt)^4}{L_3^5} + \frac{60(L-Lt)^3}{L_3^4} - \frac{30(L-Lt)^2}{L_3^3} \end{aligned} \tag{35}$$

can be derived. The extensive derivations of the equations about the Tarı-1 curve and LCA functions of the Tarı-1 curve can be found in [15] and [17].

3.4. Tarı-2 Curve

The geometrical representation of Tarı-2 curve is similar to Baykal curve, differing only by the $l_m \cong 0.428L$. The most distinct difference between the Tarı-2 curve and Baykal curve is that Tarı-2 curve has the capability of providing second-degree contact with the joining elements, which are straight lines. This capability gives curves superiority for use in road-vehicle dynamics, as shown in [12].

The curvature function of Tarı-2 curve is offered as a function of a seventh degree parabola to provide the boundary conditions given as follows (Fig. 2):

$$\begin{aligned} l &= 0 \Rightarrow k = 0, k' = 0, k'' = 0, \\ l &= l_m \Rightarrow k = 1/R, k' = 0, \\ l &= L \Rightarrow k = 0, k' = 0, k'' = 0 \end{aligned} \quad (36)$$

The final form of the curvature function is obtained as [15]

$$\begin{aligned} k_{T2}(t) &= \frac{823543}{6912R}(t^7 - 4t^6 + 6t^5 - 4t^4 + t^3), \\ & 0 \le t \le 1 \end{aligned} \quad (37)$$

By taking into account similar boundary conditions with the function of curvature, the function of superelevation can be obtained as

$$\begin{aligned} u_{T2}(t) &= \frac{823543 u_{max}}{6912}(t^7 - 4t^6 + 6t^5 - 4t^4 + t^3), \\ & 0 \le t \le 1 \end{aligned} \quad (38)$$

3.4.1. LCA Function of Tarı-2 Curve in Motion Model with Constant Velocity

By taking into consideration of Eq. 37, Eq. 38 and derivatives into Eq. 1, the LCA function of Tarı-2 curve is obtained as

$$\begin{aligned} z_{T2}(t) &= \frac{N_{T2}\nu(\nu^2 - gR\tan\alpha_m)}{LR(1 + Q_{T2}^2 \tan^2\alpha_m)^{3/2}}, \\ & 0 \le t \le 1 \end{aligned} \quad (39)$$

where

$$\begin{aligned} Q_{T2} &= \frac{823543}{6912}(t^7 - 4t^6 + 6t^5 - 4t^4 + t^3), \\ N_{T2} &= \frac{823543}{6912} \times \\ & (7t^6 - 24t^5 + 30t^4 - 16t^3 + 3t^2) \end{aligned} \quad (40)$$

The extensive derivations of the equations about the Tarı-2 curve and LCA functions of the Tarı-2 curve can be found in [15].

4. Comparison of the Curves on the Base of LCA

Curves are compared by taking into account LCA functions in motion model with constant velocity. Three criteria are used to make decisions about the curves [15, 17].

4.1. Criterion 1

The continuity of the LCA function is the most important criterion in comparisons of transition curves, because discontinuities in the form of jumps [7, 9, 12] affect travel comfort on railways and highways, and change the geometry of the rails, and more importantly cause wear on wheels and rails in railways [13, 15, 16, 17, 18].

Any curve, which does not have any discontinuity in the form of jumps in the diagram of LCA, is considered superior to other curves which have discontinuities [9, 12, 13, 15, 18]. Discontinuities in the form of jumps occur at the points where route elements with different geometry are joined. If two values of LCA functions belonging to different transition elements are identical, there is no discontinuity at the points. If these values are different, there is a discontinuity in the form of jump and it is given as

$$\Delta z(t_p) = z_j(t_p) - z_i(t_p) \quad (41)$$

where $z_i(t_p)$ and $z_j(t_p)$ are the values of LCA function belonging to the ith and jth route element at the joining point p whose arc length is l_p ($t_p = l_P/L$) [15, 17].

LCA function of curves as well as the spiral curve for motion model with constant velocity are illustrated in Fig. 5 by taking into account the following magnitudes as constant: Minimum radius of curvature at point M is R=1850m, the lengths of curves are L=1800m, $L_1=L_2=L_3=600$ m, maximum superelevation is $u_{max}=0.15$m, horizontal width of the road platform (railways) is p=1.5m and constant velocity is $\nu=250$ km/h. As seen in Fig. 5, none of the curves, except the spiral curve, has any discontinuities in the form of jumps on the diagrams of LCA function. Therefore, the Sinusoidal curve, Baykal curve, the Tarı-1 curve, and the Tarı-2 curve are equivalent according to criterion 1. However, the spiral curve

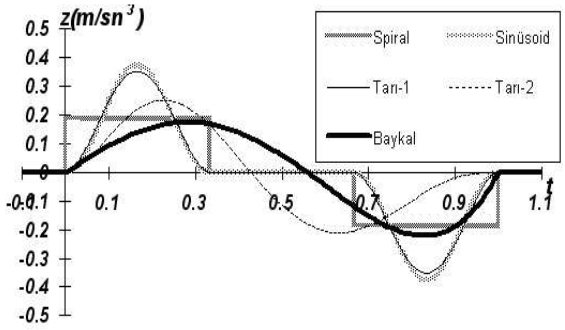

Figure 5. LCA diagram of the curve in motion model with constant velocity.

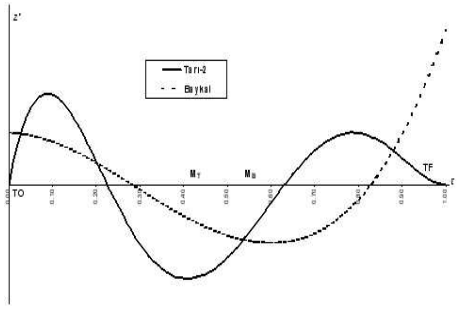

Figure 6. Diagram of the change of LCA in motion model with constant velocity.

has discontinuities in the form of jump. Therefore, the spiral curve will not be evaluated for criterion 2 and criterion 3.

4.2. Criterion 2

If the curves compared are found equivalent regarding criterion 1, then criterion 2 can be used. In order to use criterion 2, the extreme value of the function of LCA, z_e (the largest absolute value), is compared to a boundary value, z_b. Whichever transition curve satisfies the condition of

$$z_e < z_b \tag{42}$$

then the curve is assumed as superior to the curve which does not satisfy the condition of Eq. 42. Curves satisfying the condition of Eq. 42 are assumed equivalent to each other [18].

The LCA values greater than 0.3 m/sec^3 are felt by humans, and the value of 0.6 m/sec^3 is given as the limiting point at which the humans begin to feel discomfort [20, 21, 22, 31, 32, 33]. A classification can be made by taking into account the above boundary values for z_b in Eq. 42 as

$$\begin{aligned} z_e &< 0.3m/s^3 \\ 0.3m/s^3 &\leq z_e \leq 0.6m/s^3 \\ z_e &> 0.6m/s^3 \end{aligned} \tag{43}$$

As seen in Fig. 5, Baykal and Tarı-2 curves take place in the 1^{st} group in Eq. 43, therefore, they are equivalent according to the criterion 2. However, Tarı-1 curve and Sinusoidal curve are inferior curves in motion model with constant velocity according to criterion 2 and therefore will not be taken into consideration in criterion 3.

4.3. Criterion 3

The discontinuity in the form of break is defined as "the difference between the slope values of the two tangents on the diagram of LCA at the points where different route elements join "[15, 17]. The discontinuities in the form of break affect the travelling comfort and cause irregular change of LCA, although not as much as those in the form of jump. Discontinuities in the form of break take place at the points on which two different route elements join. The dynamics of the movement along the trajectory is changed by other effects such as velocity and acceleration changes. The condition for having no discontinuity in the form of break for ith and jth route elements is

$$z_i'(t_p) = z_j'(t_p) \tag{44}$$

where $z'(t_p)$ is simply derivative of the LCA function at the point P.

If the values for the two joining route elements are different, then a discontinuity in the form of break takes place and the magnitude of the discontinuity is given as [15]

$$\Delta z'(t_p) = z_j'(t_p) - z_i'(t_p) \tag{45}$$

The diagram of z' is shown in Fig. 6. The discontinuity values show that the Tarı-2 curve is superior to Baykal curve in motion model with constant velocity according to the criterion 3, because there is no discontinuity for the Tarı-2 curve although it exists for the Baykal curve.

5. Conclusion

The four new generation transition curves named as the sinusoidal curve, the Baykal curve, the Tarı-1 curve and the Tarı-2 curve are presented briefly. The sinusoidal curve and Tarı-1 curve have the ability of joining a straight line with a circular arc, whereas the Baykal curve and Tarı-2 curve have the ability of joining two straight lines without the need of a circular arc. All of the curves presented in this paper provide high order requirements of road vehicle dynamics as defined by the lateral change of acceleration function.

The LCA functions of each curve are given in motion model with constant velocity. By taking into consideration of LCA functions and the change of LCA, three criteria are defined to compare curves. The diagrams of LCA and the change of LCA for curves are plotted to make criticism by using the criteria. According to the criterion 1, all curves are determined equivalent. Sinusoidal curve and Tarı-1 curve are inferior curves with the criterion 2 and these curves are not justified for criterion 3. The Tarı-2 curve is concluded as the superior curve to the Baykal curve on the base of vehicle road dynamics defined by LCA.

References

[1] Winterhoff, Die Ausbildung von Strassenkrümmungen nach der Lemniskate (Verkehrstechnik, Germany, 1933).

[2] R. Klein, Beitrag zur Gestaltung der Übergansbögen (Gleistechnik und Fahrbahnbau, Germany, 1937)

[3] F.Birman, Gleisgeometrie und Kunstruktion des Oberbaues von Schnellfahrstrecken, ETR-Eisenbahntechnische Rundschau, Heft12, Germany, pp.513 (1968).

[4] B.K. Roy, Journal of Transportation Engineering **120**, 674 (1994) .

[5] S.K. Rao, Journal of Transportation Engineering **121**, 169 (1995) .

[6] A. Kobryn, Zeitschrift für Vermessungwesen **116**, 284 (1991).

[7] A. Kobryn, Zeitschrift für Vermessungswesen **93**, 227 (1993) .

[8] P. Schuhr, Rail International **18**, 17 (1986).

[9] D. Kahler, Vermessungstechnik und Raumordnung **52**, 10 (1990).

[10] M. Lipicnik, Journal of Transportation Engineering **124**, 546 (1998).

[11] O. Baykal, ASCE Journal of Surveying Engineering **122**, 132 (1996).

[12] E. Jacobs, Vermessung-Ingenieur **87**, 3 (1987).

[13] E. Tarı and O. Baykal, A New Transition Curve, Proc. Symp. 1^{st} Turkish-German Joint Geodetic Days, Istanbul, 1995.

[14] E. Tarı, Spline as a Route Element (In Turkish), Proc 5th Symp. on The Use of Computer in Civil Engineering, Istanbul, 1996.

[15] E. Tarı, Ph.D. Thesis, ITU (1997).

[16] E. Tarı and O. Baykal, A New Transition Curve Joining A Straight Line with A Circular Arc, Proc. Symp. Berlin, 1997.

[17] E. Tarı and O. Baykal, ARI An Interdisciplinary Journal of Physical and Engineering Sciences by Springer-Verlag **51**, 126 (1998).

[18] O. Baykal, E. Tarı, Z. Coşkun, and M. Şahin, Journal of Transportation Engineering **123**, 337 (1997).

[19] D. Kahler, Zeitschrift für Vermessungwesen **115**, 154 (1990).

[20] H.C. Ives and P. Kissam, Highway Curves (John Wiley & Sons, Inc., 1966).

[21] W. Schofield, Engineering Surveying (Butterworth - Heinemann, Oxford, 2001).

[22] O'Flaherty, C.A, Highways (Edward Arnold, London, 1986).

[23] C. Esveld, Modern Railway Track (Graphics Department of Thyssen Stahl A.G., Duisburg, 1989).

[24] D. Kahler, Vermessungstechnik und Raumordnung **51**, 116 (1989).

[25] A. Kobryn, Vermessungstechnik und Raumordnung **53**, 385 (1991).

[26] E.K. Morlok, Introduction to Transportation Engineering and Planning (McGraw-Hill, Inc., 1978).

[27] W. Gurschke, Der Vermessungsingenieur **43**, 157 (1992).

[28] R.J. Sharpe and R.W. Thorne, Computer Aided Design **14**, 79 (1982).

[29] T.E. Shoup, Applied Numerical Methods for Microcomputer (Prentice-Hall,Inc., New Jersey, 1984).

[30] W.H. Press, B.P. Flannery, S.A. Teukolsky, and W.T. Vetterling, Numerical Recipes in C, The Art of Scientific Computing, (Cambridge University Press., Cambridge, 1988).

[31] T.F. Hickerson, Route Location And Surveying (McGraw-Hill Book Company, Inc, New York, 1953).

[32] C.F. Meyer, Route Surveying, (International Textbook Company, Scranton, Pennsylvenia USA, 1965).

[33] M.C. Good, Australian Road Research **7**, 14 (1977).